

Electrospun Cellulose Acetate Membranes Coated with Polypyrrole and Their Potential Application in the Recovery of Metals

María M. Castillo-Ortega, Diego Hernández-Martínez, Irela Santos-Sauceda, Damián F. Plascencia-Martínez, Juana Alvarado-Ibarra, José L. Cabellos-Quiroz, and Yael I. Cornejo-Ramírez*



Cite This: *ACS Omega* 2022, 7, 31059–31068



Read Online

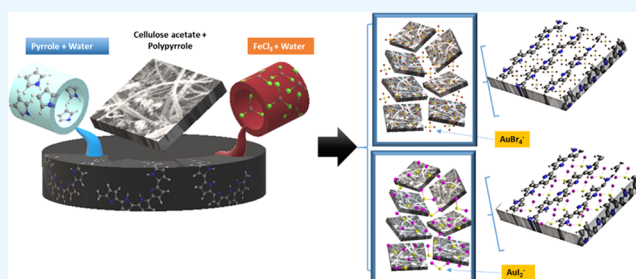
ACCESS |

Metrics & More

Article Recommendations

ABSTRACT: The purpose of this paper is to study the effect of polypyrrole (PPy) on cellulose acetate (CA) membranes prepared by the electrospinning technique (controlled variables) in the recovery of gold complexes of aqueous solutions that are environmentally ecofriendly. CA-PPy membranes were characterized by SEM, EDS, FTIR spectroscopy, contact angle measurements, electrical conductivity, and mechanical tests. They were submerged in two aqueous solutions using two gold complexes, AuI_2^- and AuBr_4^- , at room temperature. The recovery percentage was evaluated for several hours using the atomic adsorption technique for both complexes. The main findings

indicate that the percentage of recovery in the first hours of the test was very high (>80%). The adsorption efficiency maxima were similar for both complexes (91%). The Langmuir model suggests the formation of a monolayer on the surface. The electrical conductivity did not change over time, and the mechanical properties indicate reuse in several experiments. Furthermore, the theoretical analysis showed that the system is helpful at acidic pH, funding its minimum energy. It is shown in this study that the used CA-PPy membranes show adsorption, absorption, and reusable properties with the effective recovery of the complexes in the first hours. These membranes could substitute for materials that are not environmentally ecofriendly.



1. INTRODUCTION

One of water's main properties is its capacity to solubilize many compounds. Water is an essential natural resource for humans, the environment, and industry development. The result of industrialization has led to the production of large amounts of wastewater and increased disposal of heavy metals into the environment¹ due to the growth of various industries that involve metal plating, mining, painting, batteries, paper, printing, and photography, pesticides, fertilizer, etc.² The results are water pollution and scarcity in the world. On the other hand, many separation methods have been used for water remediation. Among them are treatments to remove organic (photocatalysis, adsorption with organic material, bioremediation) and inorganic (ion exchange, precipitation, coagulation and flocculation process, lixiviation, adsorption, filtration) pollutants. Nevertheless, most of these procedures involve high operational and capital costs.³

For that reason, different natural and low-cost materials have been proposed, like adsorbents such as goethite, quartz, and alumina,⁴ activated carbon,⁵ cellulosic materials,⁶ and electroconductive polymers. For example, polyaniline and PPy have both properties, adsorption and ion exchange, in their composites. Cellulose acetate (CA) is a natural polymer

demonstrating ease of processing and high mechanical properties. This polymer could be easily used like membranes, fibers, and spheres and can be used as a composite material reinforcement.^{7–9} This research uses an electroconductive polymer as an ion exchange material.

Electroconductive polymers (polyanilines, polythiophenes, and polypyrroles) exhibit excellent electrical and environmental stability but poor mechanical properties. PPy is a conducting polymer that has been extensively reported because of its varied potential applications and environmental stability, high conductivity, redox properties, and ease of synthesis.¹⁰ PPy has exhibited a promising prospect in adsorption applications because of its nitrogen atoms in the polymer chains.^{11–13} Conducting polymers are not soluble in common solvents and are difficult to cast. Usually, the conductive layer deposition on the appropriate porous support is employed to

Received: May 19, 2022

Accepted: August 12, 2022

Published: August 23, 2022



prepare a conductive polymer membrane.¹⁴ The composites of conducting polymers and some cellulosic materials have been demonstrated to be suitable adsorbents of different pollutants like heavy metals and dyes.¹⁵ In our findings, the electroconductive membranes with natural polymers ease ionic exchange and prevent environmental interaction. It is worth mentioning the significant mechanical properties that enable these membranes to be used with excellent recovery and removal efficiency once they have fulfilled their function.

The use of composite materials of electroconductive polymers to remove metals has been reported. For example, Wu et al. used polypyrrole embedded electrospun nanofibrous poly(ether sulfone) nanofibrous membranes to remove silver ions. They found adsorption of 35.7 (Ag/PPy) (mg/g).¹⁶ Wang et al. used the PAN/PPy core/shell nanofiber for Cr(VI) removal, and the adsorption amount was 65.5 mg/g at 5 h.¹⁷ Wang et al. investigated PPy-coated electrospun nanofiber mats that have been used as separation membranes to recover Au from aqueous $[\text{Au(III)Cl}_4]^-$ solutions, and they removed approximately 90% (Au(III)).¹⁸ PPy and polyaniline (PAni) were used to remove silver ions from aqueous solutions (90%).¹⁹ In a previous work, Mensah-Biney et al. evaluated the adsorption of gold–bromine species on an ion-exchange resin using a batch system.²⁰ Castillo-Ortega et al. reported a comparative study of cellulose acetate membranes (they used the phase inversion method), coated with PAni or PPy for adsorption and subsequent desorption of a gold–iodide complex; both membranes (PPy and PANI) remove about 60% of the complex.²¹ Finally, Rascón-Leon et al. used PPy coated membranes manufactured by the inversion method of phases in the recovery of the gold–bromine complex; before 10 h, the recovery reached about 40%, and after 15 h recovery stabilized at 85%.²² Composite materials in the fiber shape of electroconductive polymers have a highly porous structure with specific surface and electrochemical properties and ion exchange capacities.²³ Conductive CA/PPy composite fibers have been obtained with the great advantage of preserving the main properties of electrospun membranes (flexibility, porosity, and large surface area). The characteristics/novelities of this work are as follows: (i) CA has good chemical and mechanical properties; the former allows the PPy to coat the membrane in an oxidizing medium, and the latter adds properties to allow reuse. (ii) Our fibrous membranes increase adsorption compared to previous work using membranes manufactured by phase inversion.^{22,24,25} (iii) CA by itself is already a very adsorbent material in water but not with salts because of the additional electroconductive polymer; the application is potentiated, and ion exchange is favored.

2. MATERIAL AND METHODS

2.1. Materials. The materials used in this work included cellulose acetate powder, 39.7 wt % acetyl content, average Mn = 50 000 (Aldrich); ferric chloride ACS reagent (Fermont); 99.7% acetone (Aldrich); 98% pyrrole (Aldrich), which distilled under a vacuum in a nitrogen atmosphere before use; potassium iodide ACS reagent (Meyer); $\geq 9.8\%$ iodine ACS reagent (Meyer); 99.99% gold powder, sodium bromide (Acros), 1000 ppm gold standard (Fluka); and 1,3-dibromo-5,5-dimethylhydantoin and ammonium hydroxide (JT Baker).

2.2. Preparation of the CA Membrane Coated with PPy. The electrospinning method was used for the preparation of the fibrous membranes. The polymeric solution was prepared by dissolving CA in acetone and water. This solution

was transferred to a plastic syringe of 10 mL capacity and a syringe pump from KDS Scientific, with a flow velocity of 2.4 mL h⁻¹. A high voltage of 16 kV was applied to the polymer solution, using a high-voltage power supply (Spellman, model CZE 1000R). The distance between the needle and the collector plate was set at 15 cm (optimal conditions are in a previous work²⁶). A square aluminum plate (10 cm × 10 cm) was used as a collector.

Solutions of 0.5 M pyrrole and 0.5 M FeCl₃ were prepared for coating membranes with PPy. One by one, the membranes were immersed in 70 mL of the pyrrole solution for 5 min. Then, the membranes were removed, drained, and placed in a glass vessel containing a solution of 0.5 M FeCl₃ for 15 min. After that, the membranes were dried at room temperature for 24 h.

2.3. Characterization. The morphology and elemental content of PPy in CA fibers were characterized by scanning electron microscopy (SEM, JEOL 5410LV instrument, operated at 15 kV). The profiling technique (Sloan Dektak II) was used to understand better the surface morphology and roughness of the membranes. Fourier Transform infrared spectroscopy (FTIR)–attenuated total reflection (ATR) spectra of the fiber samples were recorded in an FT-IR Spectrometer Frontier MIR (PerkinElmer); tensile tests were measured using a universal testing machine (MINIMAT) with a load cell of 200 N using a constant displacement rate of 1 mm/min according to ASTM D1708 “Standard test method for tensile properties of plastics by use micro tensile specimens”. The electrical conductivity was measured using a tungsten electrode by the two-point method.

The contact angles of CA and CA-PPy membranes were measured at room temperature with a ChemInstruments CAM-PLUS apparatus, deionized water was used as the testing liquid, and at least ten measurements were performed on each sample to obtain the average value.

2.4. Test of Application as Ion-Exchange Composites for Metallic Complexes of Au. **2.4.1. AuI₂⁻ Leaching Solution.** The leaching solution was prepared as follows: 12 g of iodine total (I₂ + KI) was used in a KI to I₂ ratio of 2:1. The solution of the gold–iodide complex (AuI₂⁻) was prepared using the leaching solution; a predetermined amount of gold was added to achieve a 10 ppm concentration. The total Au concentration was verified by atomic absorption spectroscopy using a PerkinElmer 3110 atomic absorption spectrometer.

2.4.2. AuBr₄⁻ Leaching Solution. A synthetic gold bromide solution was prepared using reagent grade gold powder (–325 mesh, 99.99%) and reagent grade sodium bromide. A sodium bromide solution was prepared by dissolving 10.0 g of NaBr in 1000 mL of deionized water and adding 5.0 g of Geobrom 55 (dibromo dimethyl hydantoin) to this solution; 1.0 g of gold was added, and the gold was completely dissolved (about 24 h) by continuous magnetic stirring.

The composites coated with PPy were used for the metal complex adsorption tests for both leaching solutions.

2.4.3. Test. CA-PPy membranes were cut into square pieces of 1 cm × 1 cm. They were then placed into an Erlenmeyer flask and immersed in the solution of the metallic complex; constant magnetic stirring (155 rpm) was used. At the end of the test, the membranes were removed from the flask, and the final concentration of metal in the solution was determined. The composites' contact times with the metal complex solution varied in a range from 0 to 840 min. Individual experiments for each contact time were performed. In all tests, the initial Au

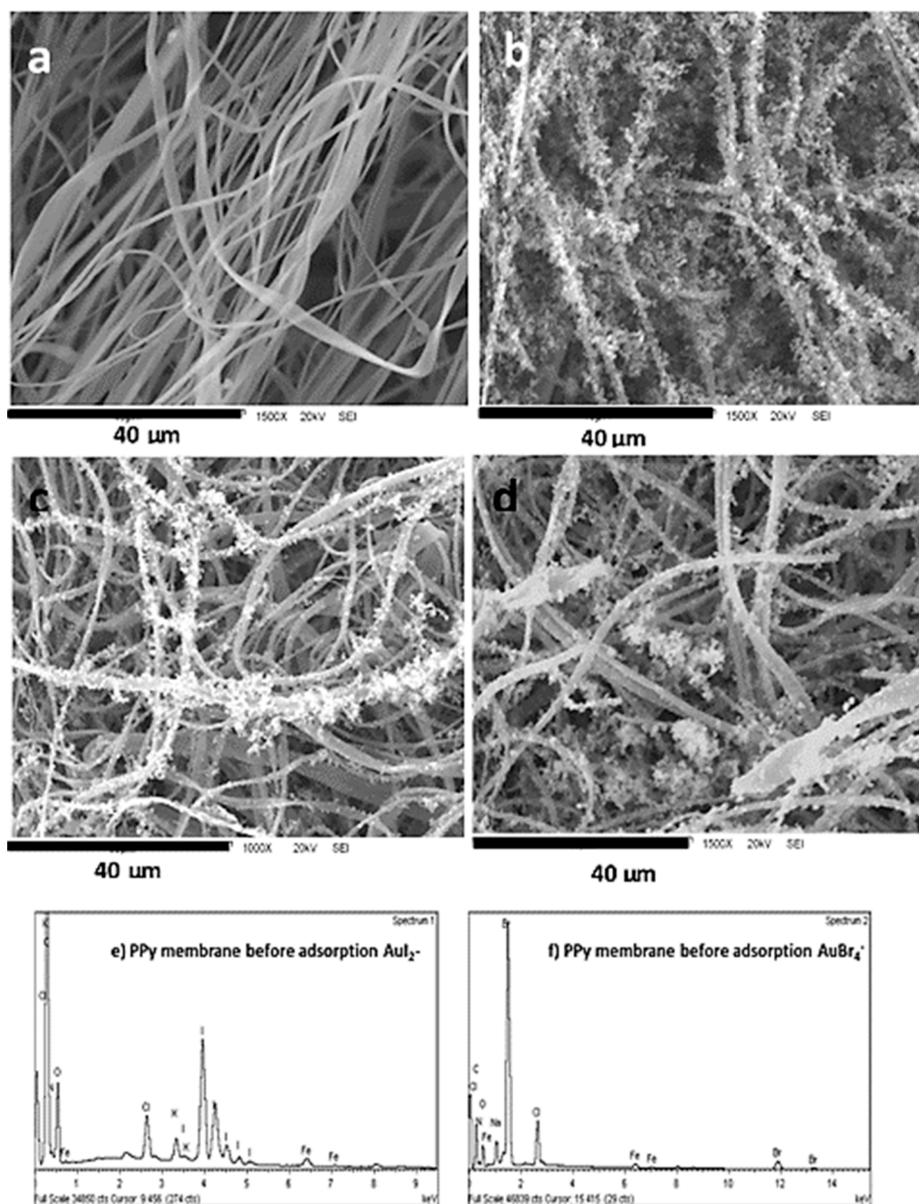


Figure 1. SEM images of (a) CA membranes, (b) CA membranes with PPy, (c) CA-PPy membranes in AuI_2^- , and (d) CA-PPy membranes in AgBr_4^- . (e and f) EDX analyses of the samples in (c) and (d).

concentration was 10 ppm. The solid/liquid ratio was 1 g L^{-1} (composite grams/liter of solution). The metal concentration was analyzed using a PerkinElmer Analyst 200 atomic absorption spectrometer. All experiments were performed in triplicate.

2.5. Equilibrium Experiments. Solutions at different concentrations (1, 5, 10, and 15 ppm) of Au were used to obtain adsorption isotherms. A membrane portion with a 2 g L^{-1} solid/liquid ratio (grams of membrane/liter of the solution) was used. The membranes were cut into pieces of $1 \text{ cm} \times 1 \text{ cm}$. These were introduced into Erlenmeyer flasks and submerged in the AuI_2^- and AuBr_4^- complex solutions under constant magnetic agitation (155 rpm) for 12 h. After this time, the membranes were immediately removed from the complex solutions. These experiments were carried out at 25°C . The concentrations of Au in the remaining solutions were analyzed by atomic absorption spectroscopy.

2.6. Desorption Test of the Metallic Complexes of Au.

The desorption experiment was performed using a $3 \text{ M NH}_4\text{OH}$ solution. The composite with a metallic complex was placed in the solution for 12 h. The concentration of the metal in the solution was determined by atomic absorption spectroscopy.

2.7. Computational Details. In the model the PPy, we used three rings and applied density functional theory (DFT),^{27,28} as it is implemented in the Gaussian 09 suite of programs,²⁹ to calculate all geometries and energies. Our procedure employs a modified-kick heuristic algorithm in Python coupled to the Gaussian 09 code to systematically explore the PES of molecular clusters formed by PPyCl^- and AuBr_2^- fragments. We used this complex to facilitate the calculation. The interested reader is referred to ref 30 for details about this metaheuristic. The optimized geometries and energies are reported at PBE0-D3/def2-TZVP/FREQ using the self-consistent reaction field (SCRf) and continuum

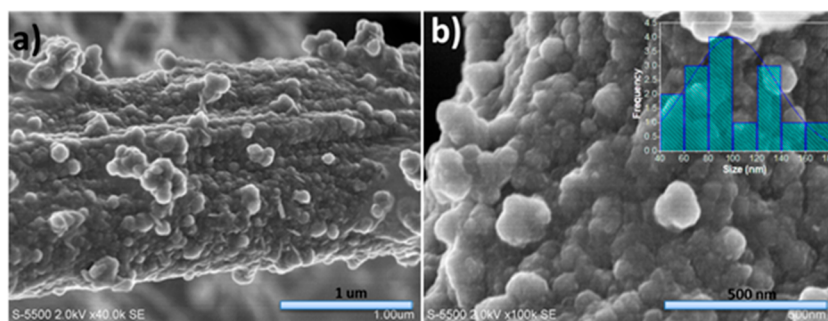


Figure 2. SEM images CA membranes with PPy at the magnification of (a) 40 KX and (b) 100 KX.

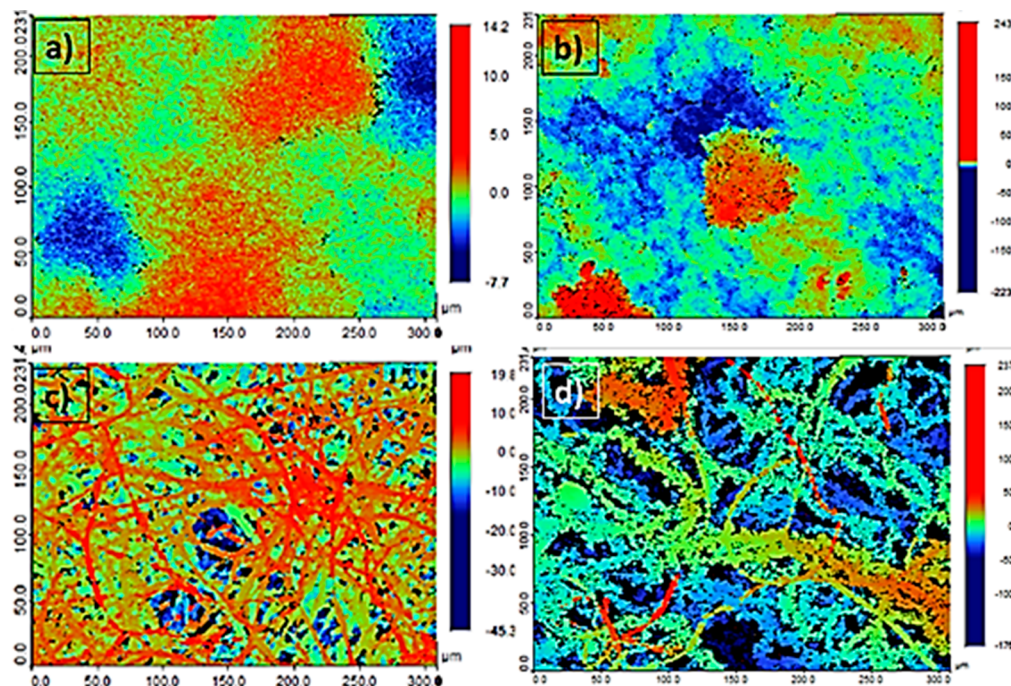


Figure 3. Surface roughness profiles of (a) the CA phase inversion, (b) the CA-PPy phase inversion, (c) CA fibers, and (d) CA-PPy fibers.

solvation model SMD,³¹ where water was used as a solvent for all the calculations. This approach includes the D3 version of Grimme's dispersion corrections,³² the PBE0 functional,³³ and the def2TZVP basis set.³⁴ To ensure that all geometries are the right minimum energy structures, we performed a frequency analysis with no imaginary frequencies presented in all arrangements reported in this work. The energy differences discussed here include the harmonic zero point energy (ZPE) correction.

3. RESULTS AND DISCUSSION

3.1. Characterization. **3.1.1. Morphology.** Figure 1 shows the SEM micrographs of CA membranes before and after coating with PPy, respectively. Figure 1a perceives the fibers' existence as like ribbons with diameters ranging from 0.2 to 0.7 μm and a smooth surface. This form agglomerates the fibers and could affect the membrane's hydrophilicity, as presented in the contact angle study. Figure 1b corresponds to CA coated with PPy, and these membranes show a coating with different size agglomerates (Figure 2b, the particles of PPy form a coating on the fibers). It should be noted that the efficiency of the adsorber membranes is due to the large contact surface area of the fibers. In this case, the nanoparticles give a

cylindrical shape to the fibers and increase the separation between them, which allows direct contact with the gold complexes, thus achieving more significant interaction and ion exchange.

Figure 1c displays the SEM micrographs of CA-PPy after the adsorption of AuI_2^- , and Figure 1d displays the SEM micrographs after the adsorption of AuBr_4^- for 12 h; both figures show agglomerates. No significant change or degradation after adsorption is observed after 12 h. The EDX analysis (Figure 1e) reveals the incorporation of iodine for the first sample due to the adsorption of this complex (AuI_2^-) on the membrane exposed for 12 h. For the AuBr_4^- complex (Figure 1f), the same happens. Instead of adsorbing the iodine complex now, bromine is adsorbed. In Figure 3 we can observe the coating of the PPy particles on the fibers, finding a particle size on the order of nanometers, which means that a system with a large surface area was obtained that enhances adsorption and chemical interactions on the membrane constructed.

3.1.2. Surface Profilometry. Figure 3 shows the surface roughness profiles of the CA membranes by phase inversion and electrospinning techniques. Figure 3a shows that the roughness is about 1.29 μm , and then when this membrane is coated with PPy, the roughness increases to 2.84 μm (Figure

3b). The CA membranes prepared by the electrospinning technique present a roughness of $3.43 \mu\text{m}$ (Figure 3c), and once they are coated with PPy this increases to 14.2 (Figure 3d). Table 1 summarizes the roughness measurements of the

Table 1. Average Roughness and Maximum Height

membrane	Ra (μm)
CA fibers	3.43
CA phase inversion	1.29
CA-PPy fibers	14.2
CA-PPy phase inversion	2.84

pure membranes coated with PPy. Physically, this last material is essential because of its large contact surface. Lu and Hsieh mention that the increase in wetting is attributed to the increase in roughness. In other words, high and intimate contact can be achieved between the membrane with more porosity and the wetting solution.³⁵ So, the wettability depends on the surface's average roughness of the material.³⁶ Another critical parameter is the roughness, and this suggests to us the idea that the incorporation of PPy on the surface helps the removal of metal complexes.

3.1.3. Contact Angle Measure. The contact angle depends upon a material's surface roughness and chemical composition. The wettability is high if the contact angle is less than 90° and the surface is hydrophilic. On the other hand, the wettability is low if the contact angle is greater than 90° and the surface is hydrophobic.³⁷

Table 2 shows the comparative results between the membranes made by electrospinning and those made by

Table 2. Contact Angle of CA Fibers, CA Phase Inversion, CA-PPy Fibers, and CA-PPy Phase Inversion

membrane	contact angle (θ)
CA fibers	$106^\circ \pm 5.11$
CA phase inversion ²²	$51.9^\circ \pm 2.9$
CA-PPy fibers	no angle
CA-PPy phase inversion ²²	$42.4^\circ \pm 1.4$

phase inversion. It can be observed that between these two membranes, the ones manufactured by electrospinning show a higher contact angle (hydrophobic). In FTIR, we observe the intense band of 1754 cm^{-1} ($\nu_{\text{C=O}}$). Zhou et al. mention that if this band is intense, the degree of acetylation of the cellulose is confirmed, and therefore the OH groups decrease (related to the polarity of the surface, which is very altered).³⁸ Therefore, their work demonstrates that if the degree of acetylation is high, the contact angle is greater (hydrophobic). Mikaeili and Gouma mention that, with the electrospinning process also, the reduction of OH groups is diminished, which increases the hydrophobicity. In our measurement, we also confirm this.³⁹ In comparison with membranes manufactured by phase inversion, it is remarkable that their porosity influences the greater hydrophilicity. When covered with PPy, we can observe how the porosity decreases in the case of membranes manufactured by phase inversion. In contrast, for those produced by electrospinning, the contact angle disappears as the membranes are absorbed by the material. This may be expected because the lone pair of valence electrons in nitrogen could induce hydrogen bonding between the heterocyclic pyrrole and water molecules, which aids in the wetting of

PPy.⁴⁰ It is confirmed that because of the roughness of the material in addition to its chemical nature, the membranes are widely wettable, which increases the contact area between the solution and the material. Ouyang and Chance et al. report that PPy content, roughness, and conductivity increase wettability.⁴¹

3.1.4. Mechanical Properties. The mechanical properties of the electrospun membranes were compared to those of membranes prepared by phase inversion,²² as shown in Table 3. The electrospun membranes show better mechanical

Table 3. Mechanical Properties of the CA Membranes by Phase Inversion and CA by the Electrospinning Method

membrane	tensile strength (MPa)	Young's modulus (MPa)	strain at break (%)
CA fibers	0.016 ± 0.011	0.356 ± 0.168	14.9 ± 1.4
CA phase inversion ²²	3.01 ± 0.99	166.93 ± 16.03	2.46 ± 0.55
CA+PPy fibers	0.40 ± 0.128	3.35 ± 1.59	22.76 ± 12.09
CA+PPy phase inversion ²²	1.15 ± 0.34	39.46 ± 2.65	7.50 ± 1.25

properties than the membranes fabricated by phase inversion due to their increase until rupture and the decrease of the elasticity of Young's modulus. When these are covered with PPy, the deformation at the break becomes greater (8%), and the elasticity of Young's modulus decreases by an order of magnitude.

3.1.5. FTIR Analysis. FTIR spectroscopy was used to confirm the presence of PPy on the membranes (Figure 4).

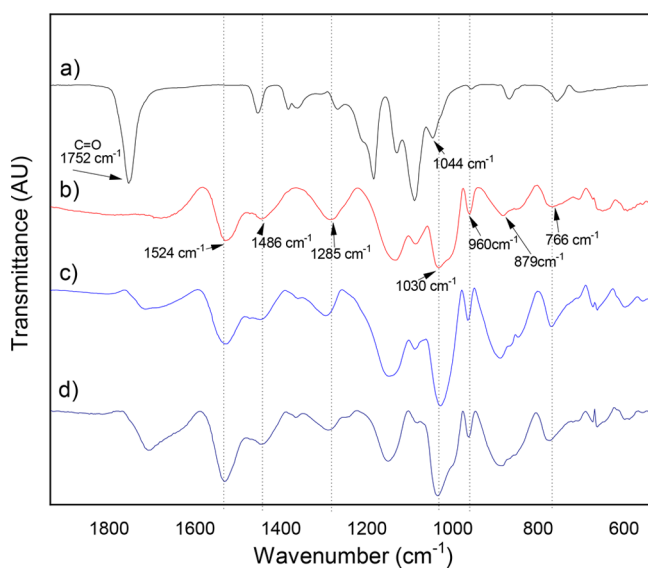


Figure 4. FTIR spectra of (a) CA membranes, (b) CA coated PPy, (c) CA-PPy AuI_2^- , and (d) CA-PPy AuBr_4^- .

The characteristic peaks of PPy are at 1524 cm^{-1} , a signal corresponding to the asymmetric ring stretching vibration of PPy, at 1486 cm^{-1} , which corresponds to the symmetric ring stretching vibration of the PPy peak, at 1285 cm^{-1} , which is associated with C–N stretching vibrations of the benzoid, and at 1030 cm^{-1} , which corresponds to the C–H deformation vibration; peaks at 960 , 879 , and 766 cm^{-1} were assigned to =C–H wagging.

3.1.6. Electrical Conductivity. Previous authors have presented evidence pointing toward a strong correlation between the nature of the anion and the PPy conductivity⁴² most likely to be ascribed to the influence of the two factors identified above, namely, the degree of polymer oxidation and film morphology.

The conductivity of CA membranes is 10^{-10} S/cm when coated with PPy. That conductivity rises to 10^{-1} S/cm. This indicates that they can be used as ion-exchange membranes. The electrical conductivity of PPy depends on the regularity of the polymer chain and interchain conductivity.⁴³

Table 4 shows the electrical conductivity measured by the two-point method (which measures the material's resistivity)

Table 4. Electrical Conductivity of the Membranes

membrane	electrical conductivity (S/cm)
Ac-PPy	$<10^{-2}$
AuBr ₄ ⁻ (1 h)	$1.64 \times 10^{-2} \pm 8.73 \times 10^{-3}$
AuBr ₄ ⁻ (3 h)	$2.66 \times 10^{-2} \pm 1.02 \times 10^{-2}$
AuBr ₄ ⁻ (6 h)	$1.39 \times 10^{-2} \pm 7.43 \times 10^{-3}$
AuBr ₄ ⁻ (12 h)	$1.43 \times 10^{-2} \pm 9.57 \times 10^{-3}$
AuI ₂ ⁻ (1 h)	$7.63 \times 10^{-2} \pm 2.99 \times 10^{-3}$
AuI ₂ ⁻ (3 h)	$9.27 \times 10^{-3} \pm 1.27 \times 10^{-2}$
AuI ₂ ⁻ (6 h)	$6.4 \times 10^{-3} \pm 1.46 \times 10^{-3}$
AuI ₂ ⁻ (12 h)	$2.13 \times 10^{-3} \pm 6.42 \times 10^{-4}$

of the membranes prepared with contact with the gold–bromine complex at 3 h. The metal ion protects the polymer against attack by water and ions, and thus the conductivity increases. In the present work, after 3 h of adsorption, an equilibrium is reached with the gold–iodine complex, and the conductivity increases an order of magnitude slightly; after 12 h, both membranes are saturated, suggesting a resistance between the polymer and the complex.

3.2. Tests of Application as Ion Exchange Membranes. Figure 5 shows the percentage of adsorption as a function of time for the membranes manufactured by the electrospinning technique and coated with PPy and uncoated.

The percentage adsorption was calculated using the following expression:

$$\% \text{ Adsorption} = \frac{(C_0 - C)}{C_0} \times 100$$

where C_0 is the initial concentration of the metal (ppm) and C is the concentration of the metal (ppm) in the solution at time t .

Previous publications have shown an adsorption percentage for AuBr₄⁻ of up to 20% at 3 h (Rascón-Leon et al.), and before the first 5 h, the adsorption percentage was below 30%;²² an AuI₂⁻ adsorption percentage below 50% at 12 h with phase inversion membranes and 97% desorption of this complex was reported.

In this work, the adsorption percentage for both complexes is about 85% in the first 3 h, reaching equilibrium after 12 h with an adsorption percentage of 90% for both complexes. This suggests that the membranes do not show selectivity specific to one of the complexes and are to be expected because it is an ion exchange that happens at the interface of the fibers that does not depend on the volume to occupy. The adsorption is fast in the first hours because of the spaces not occupied by ions; however, as time passes, these sites are already occupied, and equilibrium begins to emerge.

Yang et al. mention that the high mobility of ions (attributed to ion exchange) on the polymer matrix increases because of the incorporation of small amounts of counterions (Cl⁻, NO₃⁻, ClO₄⁻, and SO₄²⁻). Cl⁻ can be doped in the PPy chains through electronic interaction between Cl⁻ ions and nitrogen radical cations when using FeCl₃ as an oxidant.⁴⁴ This is related to the material's conductivity; i.e., if the polymer is highly doped, the conductivity increases, and therefore, the ion exchange takes place.

Figure 5 shows graphs of the adsorption percentage of the samples in AuBr₄⁻ and AuI₂⁻. As time increases, the adsorption increases until the time comes when the adsorption remains constant. Three critical characteristics encourage the adsorption of complexes on fibers. These are the morphology of the material (roughness), the conductivity, and the contact area of the coated fibers.

It should be noted that the conductivity is maintained after treatment with NH₄OH (3 M) (conductivity = 10^{-3} S/cm). The membrane can be used up to three times because it does

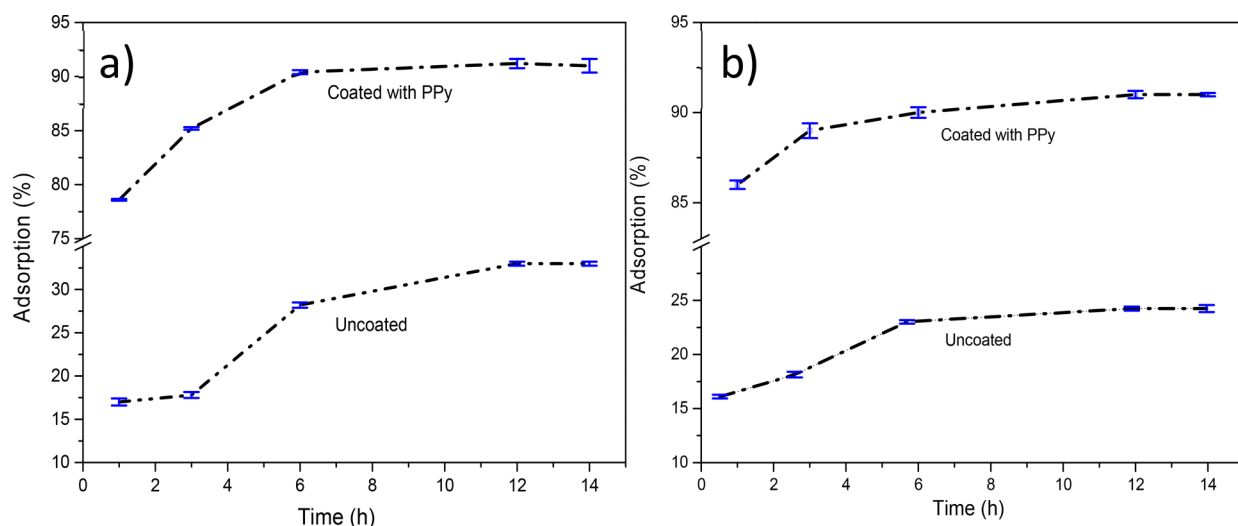


Figure 5. Adsorption kinetics of (a) AuI₂⁻ and (b) AuBr₄⁻ complexes on CA-PPy membranes; solid/liquid ratio = 10, [Au₁] = 10 ppm, $T = 25$ °C, with error bars.

Table 5. Model Parameters of Langmuir, Freundlich, and Their Corresponding Correlation Coefficients for PPy-AuI₂⁻ and PPy-AuBr₄⁻

complex	membrane	Langmuir model			Freundlich model		
		<i>K</i> (L mg ⁻¹)	<i>Q</i> _{max} (mg/g)	<i>R</i> ²	<i>c</i> ₁ (mg/g)	1/ <i>c</i> ₂	<i>R</i> ²
AuI ₂ ⁻	PPy	0.07352	4.5537	0.9954	0.4028	1.0831	0.9792
AuBr ₄ ⁻	PPY	0.9434	54.945	0.9927	4.1552	0.8417	0.9219

not show degradation until the fourth time it is used in the form of the detachment of fibers.

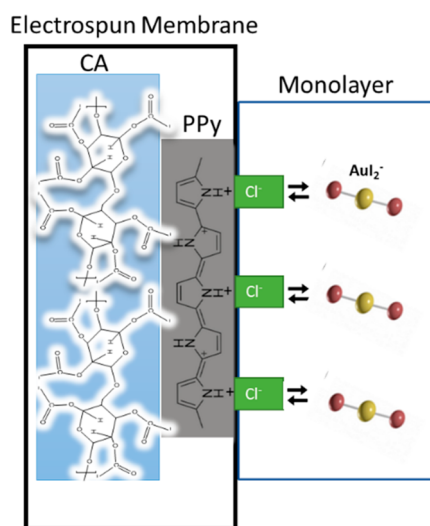
3.3. Adsorption Isotherm. Two popular isotherms, the Freundlich and Langmuir models, were applied to explore AuI₂⁻ and AuBr₄⁻ adsorptions. These isotherms are mathematical models that describe the distribution of the adsorbate species among liquid and solid phases.

The Freundlich equation, eq b, is an empirical equation based on adsorption on a heterogeneous surface. On the other hand, the Langmuir model (eq a) assumes that uptake of metal ions occurs on a homogeneous surface by monolayer adsorption without any interaction between adsorbed ions.⁴⁵ The models in the linear form are presented below:

$$\frac{C_e}{q_e} = \frac{C_e}{q_m} + \frac{1}{bq_m} \quad (a)$$

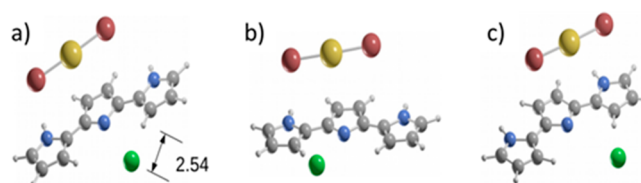
$$\ln q_e - \ln K_f + \frac{1}{n} \ln C_e \quad (b)$$

where *C_e* is the equilibrium concentration (mg/L), *q_e* is the equilibrium adsorption capacity of the adsorbent (mg/g), *q_m* is the maximum monolayer adsorption capacity (mg/g), *b* is the Langmuir parameter (L/mg), and *K_f* and 1/*n* are parameters related to adsorption capacity and surface heterogeneity, respectively. Table 5 below shows the parameters of the experiment. This suggests that both models can be applied; however, they are better suited to a Langmuir model with high *R*² values; i.e., adsorption is carried out by forming a monolayer on the surface (Figure 6). The maximum adsorption for the PPy-coated membrane in AuBr₄⁻ is 54.945 mg/g higher than that of the PPy membrane in AuI₂⁻ (4.5537 mg/g).

**Figure 6.** Schematic representation of the ion-exchange process of AuI₂⁻ on CA-PPy membranes.

3.4. Desorption Test of the Metal Complexes AuI₂⁻ and AuBr₄⁻. The membranes were subjected to a desorption test with NH₄OH (3 M), with a contact time of 12 h; both membranes achieved very similar desorption. A desorption of 73% was measured for the CA-PPy membrane that adsorbed AuI₂⁻ after the test, while in the membrane with AuBr₄⁻, the desorption was 70%. Rascón-León et al. obtained desorption with the membranes by phase inversion and PPy coated in the 54% gold–bromine complex. Although it is expected that as the interactions are weak superficially the desorption is faster, it was not entirely so.²² Electrospun membranes with large roughness due to PPy coating do not retain the complexes. This is because they form interactions only on the surface of the membranes and are only adsorbed, which does not influence the desorption process. The membranes maintain electrical conductivity for up to 5 cycles (10⁻² to 10⁻⁴ S/cm).

3.5. Optimized Geometries and Relative Energies. Figure 7 shows the three lowest energy structures in the

**Figure 7.** Lowest energy structures in the unprotonated state: (a) 0.0 kcal/mol, (b) 0.5 kcal/mol, and (c) 1.6 kcal/mol.

unprotonated state (Figure 7a). The average distance of the hydrogens to the nitrogen and carbon atoms is 1.57 Å with water as a solvent, in agreement with previous DFT calculations.⁴⁶ Our calculated distance between the chlorine and the hydrogen atoms is 2.54 Å. Also, the distance between the gold and the nitrogen atoms is 3.86 Å. Theoretical considerations on the acidity of [PPy-Cl⁻] AuI₂⁻ fragments created an unprotonated system with a deficit of protons. This deficit of protons does not allow the dissociation of the chlorine atom from the PPy under those conditions; the interchange between the chlorine and the gold atoms is not favorable.

Figure 7 shows the three optimized geometry structures for the unprotonated system. The relative Gibbs free energy is in kcal/mol. In Figure 7a, for the lowest energy structure with a relative Gibbs energy of 0.0 kcal/mol at 298.15 K, the distance between chlorine and the closet hydrogen atoms is 2.54 Å as shown. In Figure 7b is the second lowest energy structure, and Figure 7c shows where the third isomer is located. The Cl, Au, C, N, I, and H are depicted in green, yellow, gray, blue, red, and white colors, respectively, in this and the other figures. In Figure 7b, the second isomers lie just 0.5 kcal/mol above the putative minimum global. The distance between chlorine and the closet hydrogen atoms that belong to PPy is 2.53 Å. The distance between Au and the closest nitrogen of PPy is 3.85 Å. The third isomers are shown in Figure 7c 1.6 kcal/mol above

the minimum global; the Cl–H distance is 2.51 Å, and the Au–N distance is 4.0 Å. The lowest energy structure possesses the largest Cl–H distance or trend to have the largest one.

Figure 8 shows the lowest energy structures for the protonated system. In Figure 8a, we show the putative global

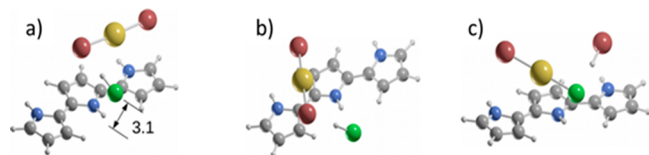


Figure 8. Lowest energy structures in the protonated state: (a) 0.0 kcal/mol, (b) 1.5 kcal/mol, and (c) 5.5 kcal/mol.

minimum where the distance between hydrogen and chlorine is 3.1 Å. In Figure 8b, the second isomers lie just 1.5 kcal/mol above the putative global minimum, and in Figure 8c, the third isomers are 5.5 kcal/mol above the global minimum. The relative Gibbs's free energies are in kcal/mol. The case of the protonated system and the lowest energy structure are shown in Figure 8, and the distance between chlorine and hydrogen in the PPy is 3.1 Å. The chlorine atom is associated with a proton forming the hydrochloric acid; also, the AuBr₂[−] complex is attracted to PPy. Our calculations showed that the system must be protonated to disassociate the Cl[−] from the PPy. The only presence of the AuI₂[−] complex is not enough to disassociate the chlorine atom (or ion). The Au–N distance is 4.0 Å. Figure 8b, we show that the second isomers lie 1.5 kcal/mol above the global minimum; also, the chlorine was able to disassociate from the PPy and form HCl, with a Au–N distance of 4.0 Å. In Figure 8c, the proton associated with one Br creates HBr, and the distance between Cl[−] and one of the hydrogens of the PPy is 2.7 Å; this system is not favorable energetically.

Figure 9 shows the lowest energy structures for the neutral (PH = 7) system. In Figure 9a, we show the putative global

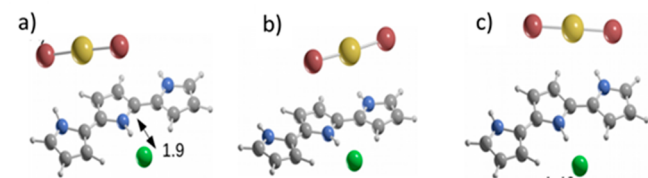


Figure 9. Lowest energy structures in the neutral state: (a) 0.0 kcal/mol, (b) 0.6 kcal/mol, and (c) 1.46 kcal/mol.

minimum where the distance between hydrogen belonging to PPy and the chlorine atoms is 1.9 Å. In Figure 9b, the second isomers lie just 0.6 kcal/mol above the putative global minimum, and in Figure 9c the third isomers are 1.46 kcal/mol above the alleged global minimum.

For the neutral case, with PH close to 7, the lowest energy structure is shown in Figure 9a, where the distance between the chlorine atom and the closest hydrogen of PPy is 1.9 Å. Our calculations indicate that the chlorine atom tends to shorten the bonding when there are no protons; the second isomers shown in Figure 9b lie at just 0.6 kcal/mol, and the HCl distance is 2.0 Å, slightly longer than in the putative global minimum. The other isomer shown in Figure 9c is located 1.46 kcal/mol above the energy of the putative global minimum,

and the HCl distance is 1.99 Å; it is clear that, in the neutral state, the chlorine does not tend to disassociate from the PPy.

4. CONCLUSIONS

Cellulose acetate membranes covered with PPy were obtained and manufactured by the electrospinning technique with controllable variables. The mechanical properties, electrical conductivity, and efficiency of adsorption and desorption of AuI₂[−] and AuBr₄[−] metal complexes give the membranes potential applications for recovering these complexes. The adsorption percentage is high (over 80%) in the early hours and stabilizes at a maximum of 90%. The recovery is attributed to the electrical conductivity of the PPy-coated membranes due to the exchange between the doping ions and the complexes. The computer modeling study found that lower energy geometry is favored with a protonated system.

Furthermore, the morphology and roughness make the surface more wettable (determined by the contact angle), and therefore, it quickly adsorbs the solution with the complexes. The adsorption isotherms determined in the equilibrium conform to the Langmuir model, suggesting that a monolayer is formed on the membrane surface. The material desorption is above 70% in both complexes, a helpful parameter indicating the reusability of the material. Electrospun membranes covered with an electroconductive polymer are viable for recovering metal complexes.

AUTHOR INFORMATION

Corresponding Author

Yael I. Cornejo-Ramírez – Departamento de Investigación y Posgrado en Alimentos, Universidad de Sonora, C.P. 83000 Hermosillo, Sonora, México; orcid.org/0000-0002-6865-0531; Email: yael.cornejo@unison.mx

Authors

María M. Castillo-Ortega – Departamento de Investigación en Polímeros y Materiales, Universidad de Sonora, C.P. 83000 Hermosillo, Sonora, México

Diego Hernández-Martínez – Departamento de Investigación en Polímeros y Materiales, Universidad de Sonora, C.P. 83000 Hermosillo, Sonora, México

Irela Santos-Sauceda – Departamento de Investigación en Polímeros y Materiales, Universidad de Sonora, C.P. 83000 Hermosillo, Sonora, México

Damián F. Plascencia-Martínez – Departamento de Investigación en Polímeros y Materiales, Universidad de Sonora, C.P. 83000 Hermosillo, Sonora, México

Juana Alvarado-Ibarra – Departamento de Investigación en Polímeros y Materiales, Universidad de Sonora, C.P. 83000 Hermosillo, Sonora, México

José L. Cabellos-Quiroz – Departamento de Investigación en Física, Universidad de Sonora, C.P. 83000 Hermosillo, Sonora, México

Complete contact information is available at:

<https://pubs.acs.org/10.1021/acsomega.2c03129>

Author Contributions

Diego Hernández-Martínez and Yael I. Cornejo-Ramírez: Methodology, Investigation, Writing-original draft. María M. Castillo-Ortega: Resources and supervision. Irela Santos-Sauceda: review and editing. Damián F. Plascencia-Martínez: review and editing. Juana Alvarado-Ibarra: Conceptualization. José L. Cabellos-Quiroz: Simulation data.

Notes

The authors declare no competing financial interest. The raw/processed data required to reproduce these findings cannot be shared at this time as the data also forms part of an ongoing study.

ACKNOWLEDGMENTS

The authors sincerely acknowledge their colleagues Silvia Burruel for SEM images and Guillermo del Carmen Tiburcio Munive for analysis of the samples by absorption spectroscopy, ACARUS(UNISON), and CONACYT-postdoctoral research 2016.

REFERENCES

- (1) Fouladgar, M.; Beheshti, M.; Sabzyan, H. Single and Binary Adsorption of Nickel and Copper from Aqueous Solutions by γ -Alumina Nanoparticles: Equilibrium and Kinetic Modeling. *J. Mol. Liq.* **2015**, *211*, 1060–1073.
- (2) Ekramul Mahmud, H. N. M.; Obidul Huq, A. K.; Yahya, R. B. The Removal of Heavy Metal Ions from Wastewater/Aqueous Solution Using Polypyrrole-Based Adsorbents: A Review. *RSC Adv.* **2016**, *6* (18), 14778–14791.
- (3) Ambaye, T. G.; Vaccari, M.; van Hullebusch, E. D.; et al. Mechanisms and adsorption capacities of biochar for the removal of organic and inorganic pollutants from industrial wastewater. *Int. J. Environ. Sci. Technol.* **2021**, *18*, 3273–3294.
- (4) Baghalha, M. The Leaching Kinetics of an Oxide Gold Ore with Iodide/Iodine Solutions. *Hydrometallurgy* **2012**, *113–114*, 42–50.
- (5) Altansukh, B.; Haga, K.; Ariunbolor, N.; Kawamura, S.; Shibayama, A. Leaching and Adsorption of Gold from Waste Printed Circuit Boards Using Iodine-Iodide Solution and Activated Carbon. *Eng. J.* **2016**, *20* (4), 29–40.
- (6) Hokkanen, S.; Bhatnagar, A.; Sillanpää, M. A Review on Modification Methods to Cellulose-Based Adsorbents to Improve Adsorption Capacity. *Water Res.* **2016**, *91*, 156–173.
- (7) Liu, C.; Bai, R. Adsorptive removal of copper ions with highly porous chitosan/cellulose acetate blend hollow fiber membranes. *J. Membr. Sci.* **2006**, *284* (1–2), 313–322.
- (8) Li, R.; Liu, L.; Yang, F. Removal of Aqueous Hg(II) and Cr(VI) Using Phytic Acid Doped Polyaniline/Cellulose Acetate Composite Membrane. *J. Hazard. Mater.* **2014**, *280*, 20–30.
- (9) Zhang, J.; Xu, H.; Guo, J.; Chen, T.; Liu, H. Superhydrophobic Polypyrrole-Coated Cigarette Filters for Effective Oil/Water Separation. *Appl. Sci. (Switzerland)* **2020**, *10* (6), 1985.
- (10) Weidlich, C.; Mangold, K. M.; Jüttner, K. Conducting Polymers as Ion-Exchangers for Water Purification. *Electrochim. Acta* **2001**, *47* (5), 741–745.
- (11) Ansari, R.; Mosayebzadeh, Z. Removal of Basic Dye Methylene Blue from Aqueous Solutions Using Sawdust and Sawdust Coated with Polypyrrole. *J. Iran. Chem. Soc.* **2010**, *7* (2), 339–350.
- (12) Bhattacharya, A.; Mukherjee, D. C.; Gohil, J. M.; Kumar, Y.; Kundu, S. Preparation, Characterization and Performance of Conducting Polypyrrole Composites Based on Polysulfone. *Desalination* **2008**, *225* (1–3), 366–372.
- (13) Ansari, R.; Keivani, M. B.; Delavar, A. F. Application of Polypyrrole Coated onto Wood Sawdust for the Removal of Carmoisine Dye from Aqueous Solutions. *J. Appl. Polym. Sci.* **2011**, *122* (2), 804–812.
- (14) Ahmed, F.; Lalia, B. S.; Kochkodan, V.; Hilal, N.; Hashaikeh, R. Electrically Conductive Polymeric Membranes for Fouling Prevention and Detection: A Review. *Desalination* **2016**, *391*, 1–15.
- (15) Fan, L.; Wei, C.; Xu, Q.; Xu, J. Polypyrrole-Coated Cotton Fabrics Used for Removal of Methylene Blue from Aqueous Solution. *J. Text. Inst.* **2017**, *108* (11), 1847–1852.
- (16) Wu, J. J.; Lee, H. W.; You, J. H.; Kau, Y. C.; Liu, S. J. Adsorption of Silver Ions on Polypyrrole Embedded Electrospun Nanofibrous Polyethersulfone Membranes. *J. Colloid Interface Sci.* **2014**, *420*, 145–151.
- (17) Wang, J.; Luo, C.; Qi, G.; Pan, K.; Cao, B. Mechanism Study of Selective Heavy Metal Ion Removal with Polypyrrole-Functionalized Polyacrylonitrile Nanofiber Mats. *Appl. Surf. Sci.* **2014**, *316* (1), 245–250.
- (18) Wang, H.; Ding, J.; Lee, B.; Wang, X.; Lin, T. Polypyrrole-Coated Electrospun Nanofiber Membranes for Recovery of Au(III) from Aqueous Solution. *J. Membr. Sci.* **2007**, *303* (1–2), 119–125.
- (19) Ansari, R.; Fallah Delavar, A. Sorption of silver ion from aqueous solutions using conducting electroactive polymers. *J. Iran. Chem. Soc.* **2008**, *5* (4), 657–668.
- (20) Mensah-Biney, R.; Hepworth, M. T.; Reid, K. J. Loading of Gold Bromo Species onto Anion Exchange Resin. *Miner. Eng.* **1993**, *6* (2), 173–191.
- (21) Castillo-Ortega, M. M.; Santos-Sauceda, I.; Encinas, J. C.; Rodriguez-Felix, D. E.; del Castillo-Castro, T.; Rodriguez-Felix, F.; Valenzuela-García, J. L.; Quiroz-Castillo, L. S.; Herrera-Franco, P. J. Adsorption and Desorption of a Gold-Iodide Complex onto Cellulose Acetate Membrane Coated with Polyaniline or Polypyrrole: A Comparative Study. *J. Mater. Sci.* **2011**, *46* (23), 7466–7474.
- (22) Rascón-Leon, S.; Castillo-Ortega, M. M.; Santos-Sauceda, I.; Munive, G. T.; Rodriguez-Felix, D. E.; Del Castillo-Castro, T.; Encinas, J. C.; Valenzuela-García, J. L.; Quiroz-Castillo, J. M.; García-Gaitan, B.; Herrera-Franco, P. J.; Alvarez-Sanchez, J.; Ramírez, J. Z.; Quiroz-Castillo, L. S. Selective Adsorption of Gold and Silver in Bromine Solutions by Acetate Cellulose Composite Membranes Coated with Polyaniline or Polypyrrole. *Polym. Bull.* **2018**, *75* (7), 3241–3265.
- (23) Deng, S.; Bai, R.; Chen, J. P. Behaviors and Mechanisms of Copper Adsorption on Hydrolyzed Polyacrylonitrile Fibers. *J. Colloid Interface Sci.* **2003**, *260* (2), 265–272.
- (24) Castillo-Ortega, M. M.; Santos-Sauceda, I.; Encinas, J. C.; Rodriguez-Felix, D. E.; del Castillo-Castro, T.; Rodriguez-Felix, F.; Valenzuela-García, J. L.; Quiroz-Castillo, L. S.; Herrera-Franco, P. J. Adsorption and desorption of a gold-iodide complex onto cellulose acetate membrane coated with polyaniline or polypyrrole: a comparative study. *J. Mater. Sci.* **2011**, *46* (23), 7466–7474.
- (25) Rodriguez, F.; Castillo-Ortega, M. M.; Encinas, J. C.; Sánchez-Corrales, V. M.; Pérez-Tello, M.; Munive, G. T. Adsorption of a gold-iodide complex (AuI_2^-) onto cellulose acetate-polyaniline membranes: Equilibrium experiments. *J. Appl. Polym. Sci.* **2009**, *113* (4), 2670–2674.
- (26) Castillo-Ortega, M. M.; Romero-García, J.; Rodríguez, F. A.; Nájera-Luna, A.; Herrera-Franco, P. Fibrous Membranes of Cellulose Acetate and Poly(Vinyl Pyrrolidone) by Electrospinning Method: Preparation and Characterization. *J. Appl. Polym. Sci.* **2010**, *116* (4), 1873–1878.
- (27) Chu, C. H.; Leung, C. W. The convolution equation of Choquet and Deny on [IN]-groups. *Integral Equ. Oper. Theory.* **2001**, *40* (4), 391–402.
- (28) Jung, J. Y.; Park, J. H.; Jeong, Y. J.; Yang, K. H.; Choi, N. K.; Kim, S. H.; Kim, W. J. Involvement of Bcl-2 Family and Caspases Cascade in Sodium Fluoride-Induced Apoptosis of Human Gingival Fibroblasts. *J. Physiol. Pharmacol. Korean.* **2006**, *10* (5), 289–295.
- (29) Barnes, E. C.; Petersson, G. A.; Montgomery, J. A.; Frisch, M. J.; Martin, J. M. L. Unrestricted Coupled Cluster and Brueckner Doubles Variations of W1 Theory. *J. Chem. Theory Comput.* **2009**, *5* (10), 2687–2693.
- (30) Guerrero-Jordan, J.; Cabellos, J. L.; Johnston, R. L.; Posada-Amarillas, A. Theoretical Investigation of the Structures of Unsupported 38-Atom CuPt Clusters. *Eur. Phys. J. B* **2018**, *91* (6), 123.
- (31) Marenich, A. V.; Cramer, C. J.; Truhlar, D. G. Universal Solvation Model Based on Solute Electron Density and on a Continuum Model of the Solvent Defined by the Bulk Dielectric Constant and Atomic Surface Tensions. *J. Phys. Chem. B* **2009**, *113* (18), 6378–6396.

(32) Grimme, S.; Antony, J.; Ehrlich, S.; Krieg, H. A Consistent and Accurate Ab Initio Parametrization of Density Functional Dispersion Correction (DFT-D) for the 94 Elements H-Pu. *J. Chem. Phys.* **2010**, *132* (15), 154104.

(33) Adamo, C.; Barone, V. Toward Reliable Density Functional Methods without Adjustable Parameters: The PBE0 Model. *J. Chem. Phys.* **1999**, *110* (13), 6158–6170.

(34) Weigend, F.; Ahlrichs, R. Balanced basis sets of split valence, triple zeta valence and quadruple zeta valence quality for H to Rn: Design and assessment of accuracy. *Phys. Chem. Chem. Phys.* **2005**, *7* (18), 3297–3305.

(35) Lu, P.; Hsieh, Y. L. Multiwalled Carbon Nanotube (MWCNT) Reinforced Cellulose Fibers by Electrospinning. *ACS Appl. Mater. Interfaces* **2010**, *2* (8), 2413–2420.

(36) Hitchcock, S. J.; Carroll, N. T.; Nicholas, M. G. Some effects of substrate roughness on wettability. *J. Mater. Sci.* **1981**, *16* (3), 714–732.

(37) Mane, A. T.; Navale, S. T.; Pawar, R. C.; Lee, C. S.; Patil, V. B. Microstructural, Optical and Electrical Transport Properties of WO₃nanoparticles Coated Polypyrrole Hybrid Nanocomposites. *Synth. Met.* **2015**, *199*, 187–195.

(38) Zhou, X.; Lin, X.; White, K. L.; Lin, S.; Wu, H.; Cao, S.; Huang, L.; Chen, L. Effect of the Degree of Substitution on the Hydrophobicity of Acetylated Cellulose for Production of Liquid Marbles. *Cellulose*. **2016**, *23* (1), 811–821.

(39) Mikaeili, F.; Gouma, P. I. Super Water-Repellent Cellulose Acetate Mats. *Sci. Rep.* **2018**, *8* (1), 12472.

(40) Teh, K.-S.; Lin, L. MEMS Sensor Material Based on Polypyrrole–Carbon Nanotube Nanocomposite: Film Deposition and Characterization. *J. Micromech. Microeng.* **2005**, *15* (11), 2019–2027.

(41) Ouyang, M.; Chance, C. M. Conductive polymer composites prepared by polypyrrole-coated poly (vinyl chloride) powder: relationship between conductivity and surface morphology. *Polymer* **1998**, *39* (10), 1857–1862.

(42) Tsai, E. W.; Pajkossy, T.; Rajeshwar, K.; Reynolds, J. R. Anion-Exchange Behavior of Polypyrrole Membranes. *J. Phys. Chem.* **1988**, *92* (12), 3560–3565.

(43) Raghunathan, S. P.; Narayanan, S.; Poulouse, A. C.; Joseph, R. Flexible Regenerated Cellulose/Polypyrrole Composite Films with Enhanced Dielectric Properties. *Carbohydr. Polym.* **2017**, *157*, 1024–1032.

(44) Yang, Z.; Peng, H.; Wang, W.; Liu, T. Crystallization Behavior of Poly(ϵ -Caprolactone)/Layered Double Hydroxide Nanocomposites. *J. Appl. Polym. Sci.* **2010**, *116* (5), 2658–2667.

(45) Shahmohammadi Kalalagh, S.; Nazemi, A. H.; Manshoury, M.; Babazadeh, H. Isotherm and Kinetic Studies on Adsorption of Pb, Zn and Cu by Kaolinite. *J. Environ. Sci.* **2011**, *9* (2), 243–255.

(46) Ullah, H.; Shah, A. U. H. A.; Bilal, S.; Ayub, K. Doping and Dedoping Processes of Polypyrrole: DFT Study with Hybrid Functionals. *J. Phys. Chem. C* **2014**, *118* (31), 17819–17830.